

The ROSAT Bright Source 1RXS J201607.0+251645: An Active Algol-type Binary

Hua-Li Li^{1,2,3}, Yuan-Gui Yang^{1,4}, Wei Su^{1,2}, Hui-Juan Wang^{1,2} and Jian-Yan Wei¹

¹ National Astronomical Observatories, Chinese Academy of Sciences, Beijing 100012, China;
lhl@bao.ac.cn

² Urumqi Observatory, Urumqi 830011;

³ Graduate University of Chinese Academy of Sciences, Beijing 100049;

⁴ School of Physics and Electric Information, HuaiBei Coal Industry Teachers College, HuaiBei 235000, Anhui Province, China

Abstract 1RXS J201607.0+251645 is identified to be an eclipsing binary. We present the preliminary observations in *V* band with the 0.6-m telescope for three years and the extensive observations in *V* and *R* band with the 0.8-m telescope for six nights, respectively. The light curve of the system is *EB* type. Five light minimum times were obtained and the orbital period of $0^d388058(\pm 0^d00044)$ is determined. The photometric solution given by the 2003-version Wilson-Devinney program suggests the binary is a semi-detached system with the photometric mass ratio $0.895(\pm 0.006)$, which probably comprises a G5 primary and an oversize K5 secondary. The less massive component has completely filled its Roche lobe, while the other almost fills its Roche lobe with the filling factor of 93.4%. The system shows a varying O'Connell effect in its phase folded diagrams from 2005 to 2007, and is X-ray luminous with $\log L_X/L_{bol} \sim -3.27$. Possible mechanisms to account for these two phenomena are discussed. Finally, we infer the binary may be in thermal oscillation or may evolve into a contact binary.

Key words: stars:binaries:close — stars: binaries: eclipsing — stars: individual: 1RXS J201607.0+251645, HD 339946

1 INTRODUCTION

Algol type binaries are eclipsing variables with the less massive component filling its Roche lobe and transferring material to its companion (Ziolkowski 1969; Proper 1989). They are X-ray emitters (Shaw & Cailiault 1996), similar to solar analogues such as RS CVn binaries (Umana et al. 1991). The driving mechanisms of X-ray emission in these systems remain unsolved though are generally thought to be related to large scale mass transfer (Sarna et al. 1998), chromospheric activity on the components (Hall 1989; Retter et al. 2005), or hot disk (Blondin et al. 1995). Finding more of them may help to shed light on their X-ray nature.

The optical variability campaign for strong X-ray sources with the 0.6-m telescope at the Xinglong observatory was launched in 2005, aiming to study long term chromospheric activity of young stars. Containing about 200 objects (much have never been identified) in the sample selected from the ROSAT bright source catalog (RBS) (Voges et al. 1999), the campaign is an excellent resource for finding new variables. 1RXS J201607.0+251645 ($\alpha_{2000.0} = 20^h16^m07.^s0, \delta_{2000.0} = 25^\circ16'45.''0$) was included in our observing program and caused our interest by its obvious eclipsing effect.

1σ positional error for 1RXS J201607.0+251645 is $9''$, including $8''$ systematic error. Within this error circle, we found a bright star HD 339946 (also known as GSC 02159-01213, TYC 2159-1213-1, and

2MASS J20160698+2516536) lying 8.8 " from the X-ray position. Thus HD 339946 is taken as the optical counterpart of 1RXS J201607.0+251645. It is listed in SIMBAD as a G5 star, with V band magnitude of 10 m .6. No previous variability description could be found in General Catalogue of Variable Stars (GCVS) (Kholopov et al. 1998) and other literature.

2 OBSERVATIONS AND THE ORBITAL PERIOD

Our first set of photometric observations of 1RXS J201607.0+251645 was performed with the 0.6-m telescope at the Xinglong observatory from Nov. 2005 to Sep. 2007. Typical observing frequency is several times per night under auto-observation mode. A PI 1024×1024 CCD and Standard Johnson V filter were used. The field of view is 17' × 17' (Xing et al. 2006).

Preliminary analysis had revealed the eclipsing effect of the target. In order to investigate its eclipsing nature in more detail, extensive observations were conducted in Nov. 2008 with the 0.8-m Tsinghua-NAOC telescope (TNT) at the Xinglong observatory. TNT employs a PI 1340×1300 CCD, giving the field of view of 11' × 11' (Zheng et al. 2008). Standard Johnson V band and R band light curves were obtained. Finding chart made from a V -band CCD image taken by the 0.8-m telescope is shown in Figure 1, with the comparison star and the check star marked as C1 and C2 (Table 1), respectively.

All photometric reductions were performed with IRAF¹ including bias and dark subtraction and flat-field correction. No differential extinction was applied since the angular distances of all the stars were small. The resulting photometric accuracy is estimated to be 0 m .01 for observations with the 0.6-m telescope and 0 m .005 for those with the 0.8-m telescope.

For preliminary observations, phase folded diagrams in Figure 2 were plotted with a period of 0 d .388 obtained with the phase dispersion minimization (PDM) method (Stellingwerf 1978).

In 2008, we obtained 648 and 645 extensive observations in V and R bands, which are shown in Figure 3 and listed in Appendix 1. The light curves vary continuously between eclipses, indicating that the system is an EB type eclipsing binary (Sterken et al. 2005). The amplitudes of various light are 0 m .52 and 0 m .51 in V and R bands, respectively. The primary eclipse is deeper than the secondary eclipse by up to 0 m .32 in V band and 0 m .29 in R band.

Five light minimum times were obtained in the extensive observations (Table 2). Using the linear least-square method, the ephemeris formula could be given as follows:

$$\text{Min.}I. = \text{HJD}2454771.6336(\pm 0.0037) + 0.388058(\pm 0.00044) \times E. \quad (1)$$

3 PHOTOMETRIC SOLUTION

The photometric solution was made with the 2003 version of Wilson-Devinney program (Wilson & Devinney 1971; Wilson 1990, 1994). Before running the DC program, a series of input parameters were fitted. The temperature of the primary component was initially set at 5160K (Cox 2000), in accordance with the G5 dwarf spectral type given in SIMBAD (operated at CDS). The gravity-darkening coefficients g_1 and g_2 were set with the same value of 0.32 (Lucy 1967), assuming convective atmospheres of the two components. The bolometric albedos were fixed as $A_1 = A_2 = 0.5$ (Rucinski 1973). Linear limb-darkening coefficients for Star 1 were $x_{1V} = 0.65$ and $x_{1R} = 0.51$, respectively (Al-Naimiy 1978). Meanwhile the limb-darkening coefficients for Star 2 (i.e., x_{2V} and x_{2R}) were determined according to its temperature T_2 . Based on the temperatures, convective atmospheres were assumed. The commonly adjustable parameters employed are the orbital inclination i , the mass ratio q , the mean temperature of Star 2 T_2 , the potential of the components Ω_1 , the monochromatic luminosity of Star 1 L_1 . The reflection effect was computed with the detailed model of Wilson (1990). The relative brightness of Star 2 was calculated by the stellar atmosphere model.

To find a photometric mass ratio, solutions were obtained for a series of trial values of the mass ratio ($q = 0.2 - 2.0$). For each value of the mass ratio, the calculation started at mode 2 (i.e., detached mode), but the solution always converged to mode 5 (i.e., semi-detached mode), suggesting the secondary has

¹ IRAF is distributed by the National Optical Astronomy Observatory, which is operated by the Association of Universities for Research in Astronomy, Inc., under cooperative agreement with the National Science Foundation.

completely filled its Roche lobe. Corresponding mass ratios and squared residuals are plotted in Fig.4, where the smallest value of $\Sigma(O - C)_i^2$ is locating at $q \sim 0.8$. At this point, the set of adjustable parameters was expanded including the mass ratio q . After a few trials and correction of mass ratio, a best-fit solution was achieved at $q = 0.895(\pm 0.006)$. The photometric elements are listed in Table 3. Synthesis light curves as solid lines are plotted in Figure 5, where the quality of the fits is fairly well in the V and R bands.

4 DISCUSSIONS

4.1 Optical variability outside eclipse

As shown in Fig.2, earlier observations had revealed the existence of O'Connell effect (Milone 1968) in 1RXS J201607.0+251645, which was varying along the time. To carefully examine how this asymmetry varied, we plot the primary maximum brightness ($Max.I$, in magnitude), the secondary maximum brightness ($Max.II$, in magnitude) and the values of $Max.II - Max.I$ of each phase folded diagram, as shown in Fig. 6. Clearly, the O'Connell effect was varying dramatically in the end of 2005: $Max.I$ was brightening by about $0.^m03$ in Nov. 2005 and $Max.II$ was darkening by about $0.^m04$ in Dec. 2005. Since 2006, the change of asymmetry became mild.

The varying O'Connell effect is also reported in other active binaries, such as GR Tauri (Gu et al. 2004), U Pegasi (Djurasevic 2001), XY UMa (Pribulla et al. 2001) and EQ Tau (Yuan & Qian 2007), in which the varying O'Connell effect is usually modeled and explained by the development and migration of hot spots (Gu et al. 2004) or dark spots (Yuan & Qian 2007; Djurasevic 2001; Pribulla et al. 2001).

So we suggest that either chromospheric activity (Strassmeier et al. 1989; Strassmeier & Bopp 1992; Strassmeier et al. 2008) or the impact of transferred mass stream onto the primary star (Pereira et al. 2006; Ibanoglu et al. 2006) is very strong in our target. Also, the actual situation is likely to be the combination of both processes.

4.2 The X-ray emission

Based on the conversion relation given by Schmitt (1995):

$$\text{flux} = (5.3 \times HR1 + 8.31) \times 10^{-12} \times \text{counts s}^{-1} [\text{erg cm}^{-2} \text{s}^{-1}] \quad (2)$$

the ROSAT count-rate of 0.111 ± 0.016 c/s and hardness ratio $HR1 = 0.07 \pm 0.13$ of 1RXS J201607.0+251645 yield a $0.1\text{-}2.4$ keV flux of $9.6 \times 10^{12} \text{ erg cm}^2 \text{ s}^{-1}$. Its distance is $19.9_{-9.6}^{+292.6}$ pc, corresponding to the parallax $\pi = 50.30 \pm 47.10$ mas (ESA 1997). Hence $\log L_X = 28.7_{-0.6}^{+2.4} \text{ erg s}^{-1}$. Combining its apparent magnitude of $10.^m6$, we got $\log L_X/L_{bol} \sim -3.27$.

Since the source is locating outside nearby molecular cloud, interstellar absorption should be marginal. As for the internal absorption, it's hard to be estimated (Feigelson et al. 2002; Stassun et al. 2004).

Our calculated $\log L_X$ is a little lower comparing to statistic values of near-contact binaries made by Shaw et al. (1996), while $\log L_X$ is in the range of 29.09 to 30.55 ergs s^{-1} . However, it is still consistent with their study, if taking into account the large uncertainty of distance. In fact, the value of $\log L_X/L_{bol}$ is more reliable, since it is independent of distance. It is falling in the high end of statistic range of -3.2 to -4.1 , suggesting the binary is X-ray luminous.

The X-ray emission in the Algol systems are generally considered to originate from chromospheric activity, interacting material, hot ($> 10^6 \text{ K}$) disk (Richards & Albright 1993; Retter et al. 2005) or extended "halo" that pervades the entire system (Siarkowski et al. 1996). Chromospheric activity is the most possible mechanism for our target. Since both components of our target are cool stars with effective temperature lower than that of the Sun, the surfaces on the two components should be in deep convective. It is generally believed that convective motions generate acoustic and MHD waves that propagate upward and heat the chromosphere and corona (Sarna et al. 1998), which can account for the strong X-ray emission in this system. If true, thus its variability outside eclipse could be easily understood, because strongly convective envelope of cool stars can also account for comparative amount of dark spots. Besides, the X-ray emission might also attribute to the interaction between infalling stream and the star (Sarna et al. 1998) or

extended "halo" that pervades the entire system (Siarkowski et al. 1996). We do not exclude their possibilities in our target, for the near-contact configuration of the system, as discussed in later section. For the mechanism of hot disk, spectral observation is needed to identify its existence or absence.

4.3 The evolutionary status

The photometric solution suggests that 1RXS J201607.0+251645 is a semi-detached binary, with the less massive component already filling up its Roche lobe. For the primary, the size of its Roche lobe can be determined according to the formula (Eggleton 1983)

$$R_L^i = \frac{0.49(m_i/m_j)^{\frac{2}{3}}}{0.6(m_i/m_j)^{\frac{2}{3}} + \ln(1 + (m_i/m_j)^{\frac{1}{3}})} \quad (3)$$

And the fill-out factor is defined as $f = r/R$ (Zhai et al. 1989), where r denotes the mean relative radius. With the above two relations, the filling factor of the primary is calculated to be 93.4%. This implies that the primary star is very close to fill up its Roche lobe. Therefore, we may infer that the two components of 1RXS J201607.0+251645 is in near-contact (Shaw 1994).

Suppose the primary is a main-sequence star, its mass and radius could be given as $M_1 = 0.92M_{\odot}$, $R_1 = 0.92R_{\odot}$ (Cox 2000), according to its spectral type G5. The secondary component should be a K5 type star, according to its temperature given by the photometric solution. Meanwhile, with mass ratio and radius ratio, we could derive the absolute parameters of the secondary as $M_2 = 0.82M_{\odot}$, $R_2 = 0.98R_{\odot}$. This calculation gives an oversize configuration to the secondary component.

Statistics show that semi-detached short-period ($P < 5d$) Algols should have lost significant amount of angular momentum (Ibanoglu et al. 2006). If angular momentum loss is continuing in this binary, we could expect that its orbital period is decreasing (Yang & Wei 2009). With the on-going mass transfer, 1RXS J201607.0+251645 may be in thermal oscillation predicted by thermal relaxation oscillation theory (Lucy & Wilson 1979). Another possibility is that it will fill up its primary component and finally evolve into a contact binary (Bradstreet & Peter 1994).

5 CONCLUSION

1RXS J201607.0+251645 is identified to an *EB* type eclipsing binary based on the morphology of its light curve. The photometric result reveals that it is a semi-contact Algol type system with the less massive component completely filling its Roche lobe. The photometric mass ratio and the orbital period are $0.895(\pm 0.006)$ and 0^d38805 , respectively. Optical variability outside eclipse of the system showed varying O'Connell effect in its phase folded light diagrams, which is likely due to hot spots generated by accretion or dark spots from chromospheric activity. The system is X-ray luminous with $\log L_X/L_{bol} \sim -3.27$. The actual process that account for its X-ray emission is not clear yet, nevertheless, possible mechanisms are discussed. The system is likely to comprise a G5 primary and an oversize K5 secondary. It may be in thermal oscillation or may evolve into a contact binary.

Acknowledgements We wish to thank the referee for suggesting a number of improvements to this paper. We are indebt to Dr. Yu-Lei QIU and Dr. Li CAO for providing original version of reduction programs. Also, we are grateful to night assistants, technical supports for their assistant of the observation, to the astronomers in the Xinglong Observatory especially Dr. Jing-Yao HU, Dr. Xiao-Jun JIANG, Dr. Jing-Song DENG and Dr. Jing WANG for helpful discussion, and to Wei-Kang ZHENG, Xu-Hui HAN and Li-Ping XIN for catching errors in our manuscript. This work was supported by the National Natural Science Foundation of China through grant No. 10778707 and No. 10473013. We have made use of the *ROSAT* data Archive of the Max-Planck-Institut fur extraterrestrische Physik at Garching, Germany, as well as the SIMBAD database, operated at CDS, Strasbourg, France.

References

- Al-Naimiy, H. M. 1978, Ap&SS, 53, 181

- Blondin, J. M., Richards, M. T., Malinowski, M. L. 1995, ApJ, 445, 939
 Bradstreet D. H., & Peter H., 1990, Bull. BBSAG, 94, 6
 Cox A. N., 2000, Allen's Astrophysical Quantities (4th ed.; New York: Springer)
 Djurasevic G., 2001, A&A, 367, 840
 Eggleton P. P., 1983, ApJL, 170, L199
 ESA 1997, The Hipparcos and Tycho Catalogues European Space Agency SP-1200 (Noordwijk:ESA)
 Feigelson E. D., Broos P., Gaffney J. A., et al., 2002, ApJ, 574, 258
 Gu S. H., Chen P. S., Choy Y. K., et al., 2004, A&A, 423, 607
 Hall D. S., 1989, Space Sci. Rev., 50, 219
 Ibanoglu C., Soydugan F., Soydugan E., Dervisoglu A., 2006, MNRAS, 373, 435
 Khlopov P. N. et al., 1998, in Combined General Catalogue of Variable stars,ver.4.1 (Moscow:Sternberg Astron.Inst.
 Lucy L. B., ApJ, 205, 208
 Lucy L. B., & Wilson R. E., 1979, ApJ, 231, 502
 Milone E.F., 1968, AJ, 73, 708
 Pereira P. C. R., Santos-Junior J. M., Pilling D. A., et al., 2006, Peremennye Zvezdy, 26, No.6
 Pribulla T., Chochol D., Heckert P. A., et al., 2001, A&A, 397, 1011
 Proper D., 1989, ApJS, 71, 595
 Qian S. B., Zhu L. Y., Boonruksar S., 2006, New Astron., 11, 503
 Retter A., Richards M. T., Wu K., 2005, ApJ, 621, 417
 Richards M. T., & Albright G. E., 1993, ApJ, 88, 199
 Rucinski S. M., 1973, ACTA ASTRO., 23, 79
 Sarna M. J., Yerli S. K., Muslimov A. G., 1998, MNRAS, 297, 760
 Schmitt J. H. M. M., Fleming T. A., Giampapa M. S., 1995, ApJ, 450, 392
 Shaw J. S., 1990, in Active Close Binaries, ed.C.Ibangolu (Dordrecht:Kluwer), 241
 Shaw J. S., 1994, Mem.Soc.Astron.Ital., 65, 95
 Shaw J. S. & Cailiault J. P., 1996, AJ, 461, 951
 Siarkowski M., Pres P., Darke S. A., et al., 1996, ApJ, 473, 470
 Stassun K. G., Ardila D. R., Barsony M., et al., 2004, AJ, 127, 3537
 Stellingwerf R. F., 1978, ApJ, 224, 584
 Strassmeier K. G., Hall D. S., Boyd L. J., et al., 1989, AJ, 69, 141
 Strassmeier K. G., & Bopp B. W., 1992, A&A, 259, 183
 Strassmeier K. G., Briguglio R., Granzer T., et al., 2008, A&A, 490, 287
 Sterken C., Jaschek C., 2005, Light Curves of Variable Stars, (Cambridge: Cambridge University Press)
 Tout C. A., Pols O. R., Eggleton P. P., Han Z., 1996, MNRAS, 281, 257
 Umana G., Catalano S., Rodono M., 1991, A&A, 249, 217
 Voges W., Aschenbach B., Boller T. et al, 1999, ApJ, 389, 405
 Wilson R. E., 1990, ApJ, 356, 613
 Wilson R. E., 1994, PASP, 106 921
 Wilson R. E., & Devinney E. J., 1971, ApJ, 166, 605
 Xing L. F., Zhang X. B., Wei J. Y., 2006, ChJAA (Chin. J. Astron. Astrophys.), 6, 716
 Yang Y. G., Qian S. B., Zhu L. Y., Liu Liang, & Nakajima K., 2008, PASJ, 60, 803
 Yang Y. G., & Wei J. Y., 2009, AJ, 137, 226
 Yuan J. Z., & Qian S. B., 2007, MNRAS, 381, 602
 Zhai D. S., Zhang X. Y., Zhang R. X., 1989, Acta Astron. Sinica, 30, 225
 Zheng W. K., Deng J. S., Zhai M., et al., 2008, ChJAA (Chin. J. Astron. Astrophys.), 8, 693
 Ziolkowski J., 1969, Ap&SS, 3, 14

Table 1 Details of target star, comparison star and check star in our observation.

star	$\alpha_{2000.0}$	$\delta_{2000.0}$	Mag(V)
target	20:16:06.98	25:16:53.8	10 ^m 6
C1	20:16:20.02	25:20:13.7	10 ^m 3
C2	20:16:06.90	25:19:21.8	11 ^m 0

Table 2 Light minimum times of 1RXS J201607.0+251645.

HJD	Band	Error
2454770.6629	R	0.0001
2454771.6314	VR	0.0002
2454774.7470	VR	0.0003
2454775.7047	VR	0.0007
2454776.6755	R	0.0004

Table 3 Light-curve solution for 1RXS J201607.0+251645.

Parameters	Values
$i(^{\circ})$	70.16(± 0.06)
$q = M_2/M_1$	0.895(± 0.006)
$T_1(K)$	5560
$T_2(K)$	4301(± 8)
Ω_1	3.7364(± 0.0118)
$\Omega_2 = \Omega_{in}$	3.5856
$L_1/(L_1 + L_2)_V$	0.8298(± 0.0070)
$L_1/(L_1 + L_2)_R$	0.7717(± 0.0056)
x_{2V}	0.85
x_{2R}	0.68
$r_1(pole)$	0.3454(± 0.0015)
$r_1(side)$	0.3602(± 0.0018)
$r_1(back)$	0.3826(± 0.0024)
$r_1(point)$	0.4116(± 0.0041)
$r_2(pole)$	0.3465(± 0.0005)
$r_2(side)$	0.3635(± 0.0006)
$r_2(back)$	0.3948(± 0.0006)
$r_2(point)$	0.4881(± 0.0022)
$\sum(O - C)_i^2$	0.1828

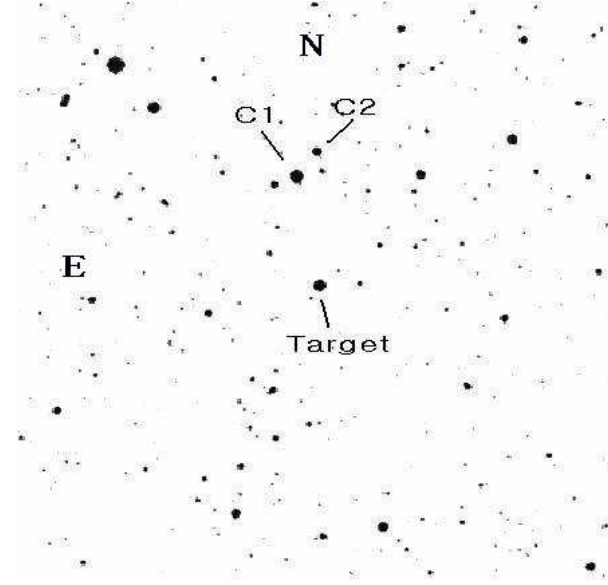


Fig. 1 Finding chart of 1RXS J201607.0+251645 made from a V band CCD image taken at the 0.8-m telescope. The field of view is $11' \times 11'$. $C1$ and $C2$ are used as comparison and check stars.

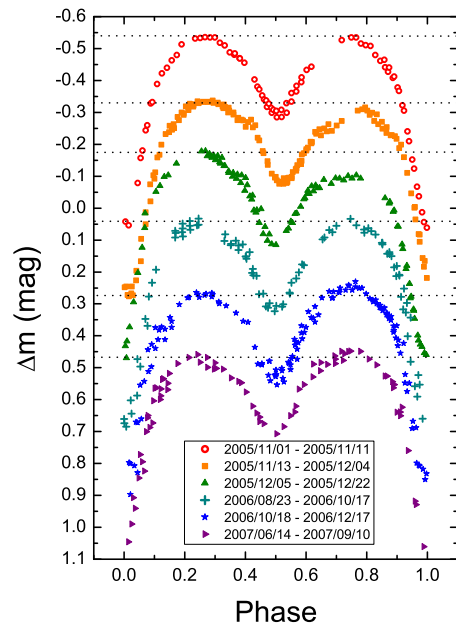


Fig. 2 Phase folded diagrams of 1RXS J201607.0+251645 from 2005 to 2007, which were made with the data obtained in the 0.6-m telescope. They are arbitrarily shifted for display purposes.

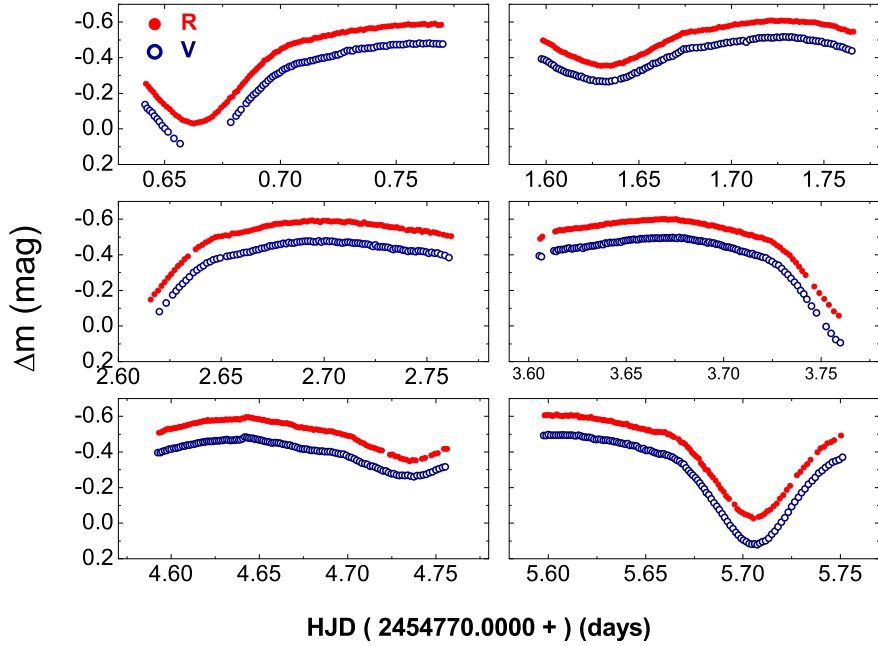


Fig.3 VR -band light curves of 1RXS J201607.0+251645 covering 6 nights with the 0.8-m telescope.

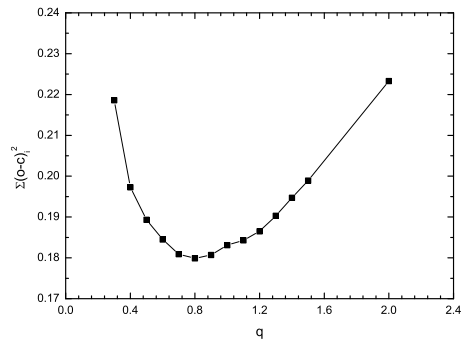


Fig.4 The relation of $\sum -q$ for 1RXS J201607.0+251645.

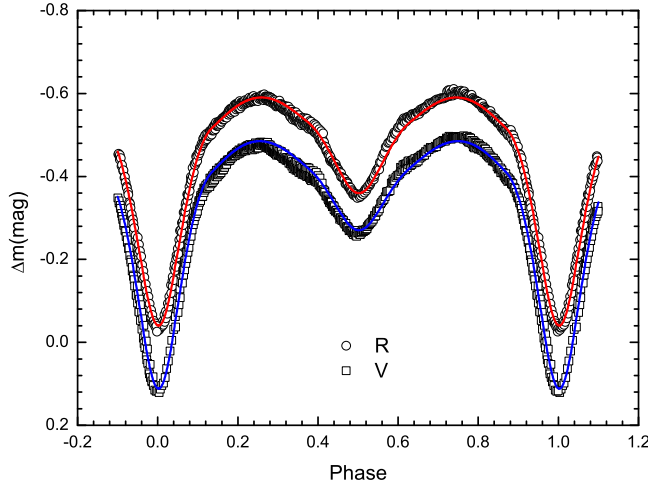


Fig. 5 Light curves of 1RXS J201607.0+251645. The open circles and squares represent V and R observations. The red and blue lines were calculated from the photometric solution.

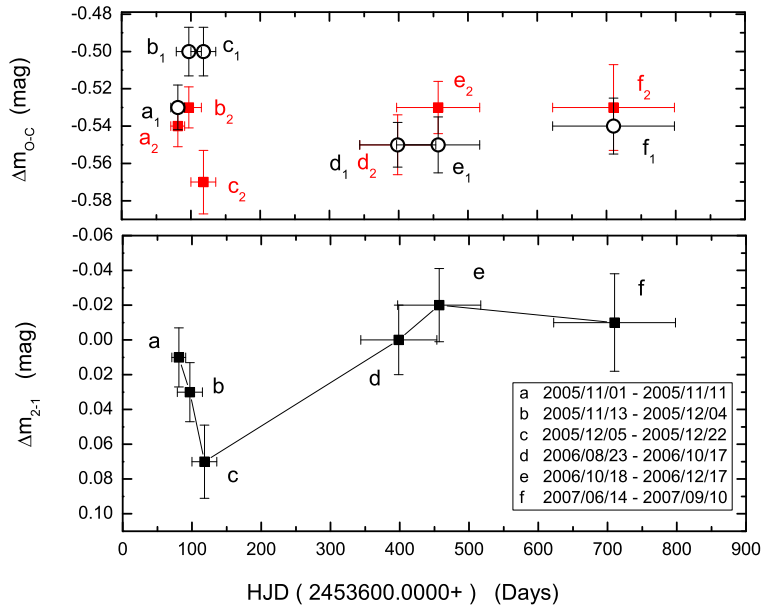


Fig. 6 The top panel: maximum brightness VS. HJD. Subscripts "1" and "2" denote the primary maximum brightness($Max.I$, in magnitude) and the secondary maximum brightness($Max.II$, in magnitude)). The bottom panel: $Max.II - Max.I$ versus HJD.

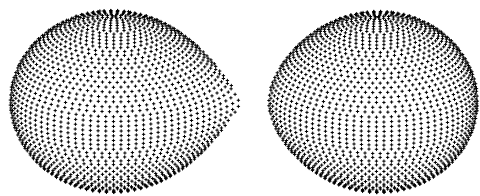


Fig. 7 3D representation for 1RXS J201607.0+251645 at phase 0.75.

I

Table .1: V band observations of 1RXS J201607.0+251645.

HJD +2454770	$\Delta(m)$								
0.6415	-0.136	0.6425	-0.116	0.6436	-0.104	0.6446	-0.091	0.6456	-0.072
0.6467	-0.057	0.6477	-0.041	0.6489	-0.018	0.6501	-0.003	0.6514	0.016
0.6540	0.053	0.6567	0.083	0.6786	-0.037	0.6808	-0.072	0.6819	-0.091
0.6830	-0.108	0.6852	-0.143	0.6863	-0.162	0.6873	-0.175	0.6884	-0.19
0.6894	-0.202	0.6905	-0.217	0.6915	-0.229	0.6925	-0.245	0.6936	-0.256
0.6946	-0.271	0.6957	-0.284	0.6967	-0.293	0.6977	-0.303	0.6988	-0.31
0.6998	-0.316	0.7008	-0.329	0.7019	-0.338	0.7029	-0.342	0.7040	-0.351
0.7050	-0.352	0.7060	-0.361	0.7071	-0.367	0.7082	-0.371	0.7094	-0.372
0.7105	-0.376	0.7117	-0.376	0.7129	-0.382	0.7141	-0.385	0.7153	-0.389
0.7165	-0.393	0.7177	-0.399	0.7189	-0.399	0.7201	-0.404	0.7213	-0.406
0.7225	-0.409	0.7237	-0.416	0.7248	-0.416	0.7260	-0.422	0.7275	-0.431
0.7288	-0.44	0.7300	-0.44	0.7313	-0.439	0.7326	-0.448	0.7339	-0.447
0.7351	-0.453	0.7364	-0.45	0.7377	-0.454	0.7389	-0.454	0.7403	-0.456
0.7417	-0.463	0.7430	-0.465	0.7444	-0.467	0.7458	-0.465	0.7473	-0.471
0.7487	-0.473	0.7501	-0.474	0.7515	-0.473	0.7530	-0.473	0.7544	-0.476
0.7558	-0.481	0.7573	-0.477	0.7587	-0.476	0.7601	-0.482	0.7616	-0.479
0.7630	-0.481	0.7644	-0.482	0.7659	-0.479	0.7673	-0.479	0.7687	-0.477
0.7702	-0.476	1.5975	-0.393	1.5988	-0.389	1.6001	-0.383	1.6015	-0.373
1.6028	-0.364	1.6041	-0.356	1.6055	-0.343	1.6068	-0.338	1.6082	-0.331
1.6095	-0.324	1.6108	-0.316	1.6122	-0.313	1.6135	-0.31	1.6148	-0.305
1.6162	-0.3	1.6175	-0.294	1.6189	-0.295	1.6202	-0.286	1.6219	-0.282
1.6236	-0.274	1.6253	-0.275	1.6269	-0.268	1.6286	-0.269	1.6303	-0.267
1.6320	-0.266	1.6337	-0.266	1.6354	-0.27	1.6371	-0.272	1.6404	-0.281
1.6419	-0.287	1.6433	-0.29	1.6448	-0.297	1.6462	-0.304	1.6477	-0.314
1.6492	-0.316	1.6506	-0.329	1.6521	-0.331	1.6535	-0.341	1.6549	-0.347
1.6563	-0.355	1.6577	-0.366	1.6592	-0.369	1.6606	-0.374	1.6620	-0.385
1.6634	-0.39	1.6651	-0.401	1.6667	-0.405	1.6684	-0.409	1.6698	-0.419
1.6713	-0.428	1.6728	-0.439	1.6743	-0.448	1.6758	-0.449	1.6773	-0.453
1.6789	-0.455	1.6811	-0.455	1.6834	-0.458	1.6853	-0.46	1.6873	-0.466
1.6890	-0.464	1.6908	-0.469	1.6925	-0.473	1.6942	-0.479	1.6959	-0.48
1.6976	-0.486	1.6993	-0.486	1.7010	-0.49	1.7028	-0.49	1.7046	-0.494
1.7064	-0.496	1.7081	-0.488	1.7100	-0.501	1.7116	-0.505	1.7132	-0.506
1.7148	-0.511	1.7164	-0.512	1.7180	-0.511	1.7197	-0.514	1.7213	-0.512
1.7229	-0.511	1.7245	-0.515	1.7261	-0.513	1.7277	-0.517	1.7294	-0.516
1.7310	-0.515	1.7326	-0.516	1.7342	-0.513	1.7358	-0.51	1.7374	-0.51
1.7391	-0.508	1.7407	-0.5	1.7423	-0.497	1.7439	-0.497	1.7455	-0.495
1.7471	-0.493	1.7488	-0.49	1.7504	-0.482	1.7520	-0.482	1.7536	-0.479
1.7553	-0.475	1.7569	-0.465	1.7585	-0.463	1.7601	-0.46	1.7617	-0.45
1.7633	-0.445	1.7650	-0.439	2.6199	-0.081	2.6232	-0.129	2.6264	-0.175
2.6280	-0.198	2.6296	-0.218	2.6312	-0.237	2.6329	-0.257	2.6345	-0.276
2.6365	-0.3	2.6382	-0.315	2.6398	-0.328	2.6414	-0.339	2.6430	-0.354
2.6446	-0.361	2.6462	-0.372	2.6479	-0.378	2.6495	-0.382	2.6527	-0.392
2.6543	-0.395	2.6559	-0.399	2.6576	-0.402	2.6592	-0.405	2.6608	-0.413
2.6623	-0.414	2.6639	-0.415	2.6654	-0.422	2.6668	-0.428	2.6682	-0.429
2.6696	-0.437	2.6710	-0.439	2.6724	-0.443	2.6737	-0.45	2.6750	-0.451
2.6763	-0.454	2.6776	-0.458	2.6789	-0.46	2.6803	-0.464	2.6816	-0.463
2.6829	-0.469	2.6842	-0.466	2.6855	-0.466	2.6868	-0.472	2.6882	-0.474

Table .1: (continued)

HJD +2454770	$\Delta(m)$								
2.6895	-0.475	2.6908	-0.477	2.6921	-0.476	2.6934	-0.476	2.6947	-0.473
2.6961	-0.473	2.6974	-0.479	2.6987	-0.472	2.7000	-0.476	2.7013	-0.479
2.7026	-0.475	2.7040	-0.477	2.7053	-0.473	2.7066	-0.47	2.7078	-0.469
2.7090	-0.467	2.7103	-0.469	2.7115	-0.471	2.7127	-0.469	2.7139	-0.466
2.7151	-0.466	2.7164	-0.466	2.7176	-0.464	2.7188	-0.461	2.7200	-0.461
2.7213	-0.46	2.7225	-0.454	2.7237	-0.447	2.7249	-0.455	2.7262	-0.446
2.7274	-0.446	2.7286	-0.445	2.7298	-0.444	2.7310	-0.441	2.7323	-0.436
2.7335	-0.43	2.7347	-0.435	2.7359	-0.434	2.7372	-0.431	2.7384	-0.427
2.7396	-0.425	2.7408	-0.42	2.7421	-0.422	2.7433	-0.421	2.7445	-0.418
2.7457	-0.422	2.7469	-0.421	2.7482	-0.42	2.7496	-0.415	2.7509	-0.408
2.7523	-0.414	2.7537	-0.408	2.7551	-0.41	2.7568	-0.402	2.7587	-0.396
2.7607	-0.384	3.6054	-0.394	3.6065	-0.389	3.6129	-0.422	3.6140	-0.42
3.6152	-0.428	3.6163	-0.429	3.6175	-0.43	3.6186	-0.431	3.6198	-0.436
3.6209	-0.438	3.6221	-0.434	3.6232	-0.437	3.6244	-0.439	3.6255	-0.44
3.6267	-0.443	3.6279	-0.437	3.6290	-0.444	3.6302	-0.446	3.6313	-0.448
3.6325	-0.451	3.6336	-0.451	3.6348	-0.454	3.6359	-0.455	3.6371	-0.46
3.6382	-0.458	3.6394	-0.466	3.6405	-0.465	3.6417	-0.47	3.6429	-0.468
3.6440	-0.47	3.6452	-0.47	3.6463	-0.473	3.6475	-0.472	3.6486	-0.479
3.6497	-0.48	3.6508	-0.482	3.6519	-0.483	3.6530	-0.485	3.6541	-0.487
3.6552	-0.486	3.6563	-0.485	3.6574	-0.49	3.6585	-0.491	3.6596	-0.491
3.6607	-0.493	3.6619	-0.49	3.6630	-0.494	3.6641	-0.493	3.6652	-0.495
3.6663	-0.494	3.6674	-0.493	3.6685	-0.495	3.6696	-0.496	3.6707	-0.495
3.6718	-0.496	3.6729	-0.495	3.6740	-0.498	3.6751	-0.495	3.6762	-0.493
3.6773	-0.497	3.6785	-0.492	3.6796	-0.494	3.6807	-0.492	3.6818	-0.487
3.6829	-0.487	3.6840	-0.486	3.6851	-0.482	3.6862	-0.48	3.6873	-0.476
3.6884	-0.479	3.6895	-0.475	3.6906	-0.473	3.6917	-0.467	3.6928	-0.471
3.6940	-0.467	3.6951	-0.466	3.6962	-0.46	3.6973	-0.46	3.6984	-0.455
3.6995	-0.45	3.7006	-0.445	3.7017	-0.444	3.7028	-0.444	3.7039	-0.439
3.7050	-0.437	3.7061	-0.432	3.7073	-0.428	3.7086	-0.42	3.7098	-0.42
3.7111	-0.416	3.7123	-0.41	3.7136	-0.405	3.7149	-0.407	3.7161	-0.399
3.7174	-0.396	3.7188	-0.392	3.7201	-0.386	3.7217	-0.383	3.7233	-0.37
3.7249	-0.361	3.7266	-0.348	3.7282	-0.341	3.7298	-0.323	3.7314	-0.304
3.7330	-0.288	3.7346	-0.268	3.7363	-0.247	3.7379	-0.227	3.7395	-0.199
3.7411	-0.181	3.7428	-0.151	3.7451	-0.113	3.7476	-0.073	3.7526	0.003
3.7551	0.042	3.7576	0.076	3.7600	0.093	4.5924	-0.396	4.5937	-0.396
4.5949	-0.402	4.5962	-0.407	4.5975	-0.408	4.5987	-0.415	4.6000	-0.415
4.6013	-0.421	4.6026	-0.421	4.6038	-0.424	4.6051	-0.428	4.6064	-0.433
4.6076	-0.434	4.6089	-0.438	4.6102	-0.438	4.6114	-0.441	4.6127	-0.443
4.6140	-0.447	4.6153	-0.45	4.6165	-0.453	4.6178	-0.455	4.6189	-0.456
4.6201	-0.459	4.6212	-0.459	4.6223	-0.459	4.6234	-0.46	4.6246	-0.462
4.6257	-0.463	4.6268	-0.462	4.6280	-0.464	4.6291	-0.465	4.6302	-0.468
4.6314	-0.47	4.6325	-0.466	4.6337	-0.464	4.6348	-0.467	4.6360	-0.466
4.6371	-0.469	4.6383	-0.468	4.6394	-0.469	4.6406	-0.475	4.6417	-0.483
4.6429	-0.482	4.6440	-0.479	4.6452	-0.476	4.6464	-0.476	4.6475	-0.472
4.6487	-0.471	4.6498	-0.468	4.6510	-0.466	4.6521	-0.463	4.6533	-0.46
4.6545	-0.458	4.6557	-0.455	4.6570	-0.451	4.6582	-0.452	4.6595	-0.452
4.6607	-0.45	4.6619	-0.448	4.6633	-0.443	4.6647	-0.442	4.6660	-0.439
4.6674	-0.439	4.6688	-0.432	4.6702	-0.43	4.6716	-0.425	4.6730	-0.419
4.6743	-0.418	4.6757	-0.415	4.6771	-0.415	4.6785	-0.41	4.6799	-0.409

Table .1: (continued)

Table .2: *R* band observations of 1RXS J201607.0+251645.

HJD +2454770	$\Delta(m)$								
0.6420	-0.253	0.6431	-0.236	0.6441	-0.22	0.6452	-0.207	0.6462	-0.187
0.6472	-0.172	0.6483	-0.157	0.6496	-0.14	0.6509	-0.124	0.6522	-0.11
0.6535	-0.093	0.6548	-0.078	0.6561	-0.066	0.6575	-0.052	0.6588	-0.046
0.6601	-0.04	0.6614	-0.034	0.6627	-0.03	0.6641	-0.036	0.6654	-0.039
0.6667	-0.042	0.6680	-0.049	0.6693	-0.058	0.6706	-0.069	0.6719	-0.086
0.6731	-0.099	0.6744	-0.119	0.6757	-0.135	0.6769	-0.15	0.6782	-0.173
0.6793	-0.182	0.6804	-0.205	0.6815	-0.213	0.6826	-0.235	0.6837	-0.252
0.6847	-0.265	0.6858	-0.283	0.6869	-0.3	0.6880	-0.315	0.6890	-0.326
0.6900	-0.341	0.6911	-0.354	0.6921	-0.365	0.6931	-0.384	0.6942	-0.391
0.6952	-0.4	0.6963	-0.41	0.6973	-0.427	0.6983	-0.433	0.6994	-0.437
0.7004	-0.45	0.7015	-0.456	0.7025	-0.463	0.7035	-0.472	0.7046	-0.475
0.7056	-0.48	0.7066	-0.484	0.7077	-0.487	0.7088	-0.49	0.7100	-0.498
0.7111	-0.497	0.7123	-0.498	0.7135	-0.501	0.7147	-0.511	0.7160	-0.511
0.7172	-0.514	0.7184	-0.522	0.7196	-0.522	0.7208	-0.528	0.7220	-0.526
0.7232	-0.532	0.7244	-0.537	0.7255	-0.538	0.7268	-0.544	0.7282	-0.542
0.7295	-0.549	0.7308	-0.553	0.7320	-0.551	0.7333	-0.554	0.7346	-0.558
0.7359	-0.556	0.7371	-0.562	0.7384	-0.565	0.7397	-0.566	0.7410	-0.564
0.7424	-0.569	0.7438	-0.573	0.7452	-0.575	0.7466	-0.576	0.7480	-0.578
0.7495	-0.582	0.7509	-0.579	0.7523	-0.582	0.7538	-0.585	0.7552	-0.588
0.7566	-0.585	0.7580	-0.585	0.7595	-0.587	0.7609	-0.588	0.7623	-0.59
0.7638	-0.584	0.7652	-0.589	0.7666	-0.591	0.7681	-0.583	0.7695	-0.585
1.5982	-0.498	1.5995	-0.49	1.6009	-0.484	1.6022	-0.476	1.6035	-0.47
1.6049	-0.455	1.6062	-0.447	1.6075	-0.438	1.6089	-0.432	1.6102	-0.428
1.6116	-0.418	1.6129	-0.413	1.6142	-0.407	1.6156	-0.403	1.6169	-0.394
1.6182	-0.391	1.6196	-0.382	1.6212	-0.378	1.6228	-0.374	1.6245	-0.367
1.6262	-0.364	1.6279	-0.356	1.6296	-0.355	1.6313	-0.357	1.6330	-0.356
1.6346	-0.355	1.6363	-0.359	1.6380	-0.365	1.6397	-0.37	1.6413	-0.368
1.6427	-0.379	1.6442	-0.384	1.6456	-0.393	1.6471	-0.397	1.6485	-0.401
1.6500	-0.413	1.6515	-0.42	1.6529	-0.423	1.6544	-0.432	1.6558	-0.44
1.6572	-0.45	1.6586	-0.459	1.6600	-0.466	1.6614	-0.474	1.6628	-0.476
1.6642	-0.489	1.6659	-0.498	1.6676	-0.504	1.6692	-0.513	1.6707	-0.521
1.6722	-0.528	1.6737	-0.539	1.6752	-0.54	1.6767	-0.543	1.6782	-0.548
1.6804	-0.546	1.6826	-0.552	1.6845	-0.555	1.6865	-0.557	1.6882	-0.557
1.6900	-0.56	1.6917	-0.564	1.6934	-0.572	1.6952	-0.571	1.6969	-0.575
1.6985	-0.578	1.7002	-0.582	1.7019	-0.589	1.7037	-0.587	1.7055	-0.592
1.7073	-0.591	1.7090	-0.594	1.7109	-0.597	1.7125	-0.598	1.7141	-0.603
1.7158	-0.601	1.7174	-0.603	1.7190	-0.605	1.7206	-0.61	1.7222	-0.609
1.7238	-0.605	1.7255	-0.605	1.7271	-0.609	1.7287	-0.608	1.7303	-0.608
1.7319	-0.605	1.7336	-0.603	1.7352	-0.605	1.7368	-0.6	1.7384	-0.602
1.7400	-0.6	1.7416	-0.598	1.7433	-0.599	1.7449	-0.599	1.7465	-0.595
1.7481	-0.59	1.7497	-0.587	1.7514	-0.585	1.7530	-0.583	1.7546	-0.579
1.7562	-0.576	1.7578	-0.566	1.7594	-0.56	1.7611	-0.558	1.7627	-0.55
1.7643	-0.544	1.7659	-0.546	2.6157	-0.149	2.6175	-0.178	2.6193	-0.2
2.6209	-0.226	2.6225	-0.247	2.6241	-0.271	2.6257	-0.291	2.6273	-0.315
2.6290	-0.338	2.6306	-0.355	2.6322	-0.375	2.6338	-0.392	2.6375	-0.431
2.6391	-0.446	2.6407	-0.456	2.6424	-0.469	2.6440	-0.479	2.6456	-0.491
2.6472	-0.499	2.6488	-0.503	2.6504	-0.504	2.6521	-0.51	2.6537	-0.509
2.6553	-0.52	2.6569	-0.521	2.6585	-0.522	2.6601	-0.525	2.6617	-0.53
2.6632	-0.532	2.6648	-0.538	2.6663	-0.543	2.6677	-0.547	2.6691	-0.551

Table .2: (continued)

HJD +2454770	$\Delta(m)$								
2.6704	-0.559	2.6718	-0.563	2.6731	-0.564	2.6745	-0.566	2.6758	-0.572
2.6771	-0.575	2.6784	-0.575	2.6797	-0.577	2.6810	-0.582	2.6824	-0.578
2.6837	-0.578	2.6850	-0.581	2.6863	-0.584	2.6876	-0.582	2.6889	-0.585
2.6903	-0.59	2.6916	-0.587	2.6929	-0.591	2.6942	-0.594	2.6955	-0.589
2.6968	-0.59	2.6981	-0.583	2.6995	-0.591	2.7008	-0.591	2.7021	-0.59
2.7034	-0.587	2.7047	-0.588	2.7060	-0.588	2.7073	-0.589	2.7085	-0.585
2.7098	-0.581	2.7110	-0.586	2.7122	-0.588	2.7134	-0.585	2.7147	-0.584
2.7159	-0.581	2.7171	-0.575	2.7183	-0.575	2.7195	-0.583	2.7208	-0.575
2.7220	-0.573	2.7232	-0.571	2.7244	-0.57	2.7257	-0.568	2.7269	-0.569
2.7281	-0.568	2.7293	-0.561	2.7306	-0.561	2.7318	-0.556	2.7330	-0.556
2.7342	-0.553	2.7354	-0.555	2.7367	-0.548	2.7379	-0.548	2.7403	-0.538
2.7416	-0.542	2.7428	-0.54	2.7440	-0.534	2.7452	-0.54	2.7465	-0.539
2.7477	-0.529	2.7489	-0.534	2.7503	-0.532	2.7517	-0.523	2.7531	-0.527
2.7545	-0.524	2.7559	-0.519	2.7579	-0.514	2.7598	-0.509	2.7617	-0.504
3.6060	-0.491	3.6071	-0.503	3.6135	-0.531	3.6146	-0.535	3.6158	-0.54
3.6169	-0.538	3.6181	-0.538	3.6192	-0.543	3.6204	-0.544	3.6215	-0.543
3.6227	-0.546	3.6239	-0.55	3.6250	-0.55	3.6262	-0.549	3.6273	-0.552
3.6285	-0.554	3.6296	-0.554	3.6308	-0.556	3.6319	-0.561	3.6331	-0.56
3.6342	-0.564	3.6354	-0.561	3.6365	-0.567	3.6377	-0.568	3.6389	-0.571
3.6400	-0.576	3.6412	-0.576	3.6423	-0.574	3.6435	-0.579	3.6446	-0.579
3.6458	-0.582	3.6469	-0.584	3.6481	-0.586	3.6492	-0.585	3.6503	-0.586
3.6514	-0.588	3.6525	-0.589	3.6536	-0.588	3.6547	-0.588	3.6558	-0.59
3.6569	-0.591	3.6580	-0.593	3.6591	-0.595	3.6603	-0.594	3.6614	-0.595
3.6625	-0.596	3.6636	-0.595	3.6647	-0.599	3.6658	-0.598	3.6669	-0.598
3.6680	-0.6	3.6691	-0.601	3.6702	-0.601	3.6713	-0.597	3.6724	-0.599
3.6735	-0.599	3.6746	-0.598	3.6757	-0.6	3.6769	-0.595	3.6780	-0.592
3.6791	-0.594	3.6802	-0.589	3.6813	-0.588	3.6824	-0.589	3.6835	-0.586
3.6846	-0.584	3.6857	-0.581	3.6868	-0.582	3.6879	-0.576	3.6890	-0.575
3.6901	-0.575	3.6912	-0.569	3.6923	-0.564	3.6935	-0.565	3.6946	-0.565
3.6957	-0.561	3.6968	-0.559	3.6979	-0.553	3.6990	-0.554	3.7001	-0.55
3.7012	-0.543	3.7023	-0.543	3.7034	-0.543	3.7045	-0.537	3.7056	-0.536
3.7069	-0.529	3.7081	-0.532	3.7093	-0.525	3.7105	-0.518	3.7118	-0.515
3.7131	-0.51	3.7143	-0.514	3.7156	-0.505	3.7169	-0.499	3.7181	-0.498
3.7195	-0.497	3.7210	-0.489	3.7226	-0.483	3.7242	-0.478	3.7258	-0.467
3.7275	-0.453	3.7291	-0.441	3.7307	-0.425	3.7323	-0.413	3.7339	-0.399
3.7355	-0.376	3.7372	-0.356	3.7388	-0.334	3.7404	-0.309	3.7421	-0.287
3.7466	-0.222	3.7491	-0.186	3.7516	-0.152	3.7541	-0.119	3.7566	-0.083
3.7591	-0.058	4.5931	-0.509	4.5944	-0.511	4.5957	-0.519	4.5969	-0.525
4.5982	-0.53	4.5995	-0.528	4.6007	-0.532	4.6020	-0.534	4.6033	-0.536
4.6046	-0.541	4.6058	-0.542	4.6071	-0.546	4.6084	-0.548	4.6096	-0.553
4.6109	-0.555	4.6122	-0.56	4.6134	-0.563	4.6147	-0.564	4.6160	-0.568
4.6172	-0.57	4.6184	-0.574	4.6196	-0.572	4.6207	-0.579	4.6218	-0.574
4.6230	-0.578	4.6241	-0.577	4.6252	-0.58	4.6264	-0.578	4.6275	-0.578
4.6286	-0.579	4.6298	-0.58	4.6309	-0.583	4.6320	-0.582	4.6332	-0.584
4.6343	-0.582	4.6355	-0.583	4.6366	-0.585	4.6378	-0.585	4.6389	-0.582
4.6401	-0.588	4.6412	-0.589	4.6424	-0.596	4.6436	-0.595	4.6447	-0.594
4.6459	-0.592	4.6470	-0.589	4.6482	-0.587	4.6493	-0.585	4.6505	-0.583
4.6516	-0.579	4.6528	-0.58	4.6540	-0.575	4.6552	-0.575	4.6564	-0.569
4.6577	-0.57	4.6589	-0.57	4.6602	-0.569	4.6614	-0.566	4.6627	-0.563

Table .2: (continued)

HJD +2454770	$\Delta(m)$								
4.6641	-0.56	4.6655	-0.562	4.6669	-0.557	4.6683	-0.555	4.6696	-0.549
4.6710	-0.542	4.6724	-0.537	4.6738	-0.54	4.6752	-0.535	4.6766	-0.534
4.6780	-0.53	4.6793	-0.53	4.6807	-0.524	4.6821	-0.527	4.6836	-0.524
4.6850	-0.522	4.6865	-0.52	4.6879	-0.515	4.6894	-0.517	4.6909	-0.516
4.6924	-0.511	4.6939	-0.506	4.6954	-0.504	4.6970	-0.499	4.6985	-0.496
4.7000	-0.49	4.7015	-0.489	4.7030	-0.483	4.7045	-0.471	4.7060	-0.462
4.7075	-0.454	4.7090	-0.448	4.7105	-0.438	4.7120	-0.432	4.7135	-0.427
4.7150	-0.423	4.7165	-0.417	4.7180	-0.411	4.7195	-0.408	4.7240	-0.384
4.7255	-0.386	4.7271	-0.375	4.7286	-0.373	4.7302	-0.364	4.7318	-0.36
4.7334	-0.357	4.7351	-0.348	4.7369	-0.355	4.7386	-0.353	4.7421	-0.361
4.7439	-0.366	4.7475	-0.381	4.7493	-0.389	4.7511	-0.393	4.7547	-0.418
4.7564	-0.417	5.5982	-0.605	5.5995	-0.608	5.6008	-0.608	5.6021	-0.602
5.6033	-0.605	5.6046	-0.611	5.6057	-0.604	5.6069	-0.602	5.6081	-0.602
5.6092	-0.605	5.6104	-0.603	5.6115	-0.607	5.6127	-0.604	5.6138	-0.604
5.6150	-0.605	5.6161	-0.594	5.6173	-0.597	5.6184	-0.594	5.6196	-0.594
5.6207	-0.591	5.6219	-0.597	5.6230	-0.589	5.6242	-0.586	5.6254	-0.583
5.6265	-0.583	5.6277	-0.58	5.6288	-0.58	5.6300	-0.576	5.6311	-0.574
5.6323	-0.576	5.6334	-0.569	5.6346	-0.564	5.6357	-0.562	5.6369	-0.56
5.6380	-0.557	5.6392	-0.555	5.6404	-0.558	5.6415	-0.547	5.6427	-0.545
5.6438	-0.538	5.6450	-0.541	5.6461	-0.535	5.6473	-0.53	5.6484	-0.53
5.6496	-0.528	5.6507	-0.521	5.6519	-0.523	5.6530	-0.515	5.6542	-0.514
5.6553	-0.512	5.6565	-0.514	5.6577	-0.511	5.6588	-0.51	5.6600	-0.512
5.6611	-0.501	5.6623	-0.499	5.6634	-0.491	5.6646	-0.483	5.6669	-0.472
5.6680	-0.455	5.6692	-0.452	5.6703	-0.444	5.6715	-0.428	5.6727	-0.415
5.6738	-0.397	5.6750	-0.386	5.6761	-0.373	5.6773	-0.363	5.6784	-0.338
5.6796	-0.324	5.6807	-0.303	5.6819	-0.297	5.6831	-0.276	5.6845	-0.258
5.6859	-0.24	5.6873	-0.216	5.6886	-0.194	5.6900	-0.177	5.6914	-0.153
5.6928	-0.137	5.6956	-0.105	5.6970	-0.079	5.6983	-0.066	5.6997	-0.059
5.7011	-0.049	5.7025	-0.044	5.7039	-0.037	5.7053	-0.026	5.7080	-0.036
5.7094	-0.041	5.7109	-0.051	5.7124	-0.067	5.7140	-0.075	5.7157	-0.094
5.7173	-0.111	5.7189	-0.138	5.7206	-0.158	5.7224	-0.188	5.7242	-0.21
5.7276	-0.269	5.7294	-0.288	5.7311	-0.313	5.7329	-0.332	5.7346	-0.357
5.7381	-0.399	5.7398	-0.421	5.7416	-0.429	5.7433	-0.449	5.7451	-0.456
5.7468	-0.467	5.7503	-0.492						